

Interaction effects on dynamical localization in driven helium

Felix Jörder, Klaus Zimmermann, Alberto Rodriguez, and Andreas Buchleitner*

Physikalisches Institut, Albert-Ludwigs-Universität Freiburg, Hermann-Herder-Straße 3, D-79104, Freiburg, Germany

Dynamical localization prevents driven atomic systems from fast fragmentation by hampering the excitation process. We present numerical simulations within a collinear model of microwave-driven helium Rydberg atoms and prove that dynamical localization survives the impact of electron-electron interaction, even for doubly excited states in the presence of fast autoionization. We conclude that the effect of electron-electron repulsion on localization can be described by an appropriate rescaling of the atomic level density and of the external field with the strength of the interaction.

PACS numbers: 32.80.Rm, 05.60.Gg, 32.80.Zb, 72.15.Rn

Anderson localization implies the exponential decay of wavefunctions in configuration space due to a disordered potential landscape [1], and is well understood as a single-particle effect [2–7]. *Dynamical localization*, its analogue emerging in periodically driven quantum systems [8], is best known in connection with the quantum kicked rotor, which has enjoyed quite an experimental success in the field of cold atoms [9–14]. There, a pseudo-randomness generated by the kicked dynamics leads to an exponential suppression of transitions to high momentum states. In the context of electromagnetically driven atomic systems, the excitation energy takes the role of the localized observable: excitation processes corresponding to an energy exchange of $E = k\omega$ exhibit an exponential decrease $\exp(-|k|/\xi)$, where $|k|$ is the net number of exchanged photons and ξ is the localization length [15–19]. The onset of localization requires processes of sufficiently high order k and the atomic level spacing to be small as compared to the photon energy ω . In this regime, the suppression of the excitation process translates into highly enhanced values of the critical field strength F^C needed to ionize the atoms with respect to the classical prediction. This effect has been measured experimentally [16, 20, 21] and is supported by numerical simulations [19, 22] for hydrogen and alkali atoms, and also by our results on collinear helium, which show a significant agreement with the experimental data (cp. Fig. 1).

In this letter we approach the problem on how localization is affected by particle-particle interactions. This is a broad-interest question which is currently being intensively investigated in the context of metal-insulator transitions and many-body Anderson localization [23–27]. The study of dynamical localization in interacting systems provides valuable information from a different perspective. Moreover, understanding the influence of electron-electron interaction in driven systems proves essential to unravel the correlations observed in laser-driven atomic ionization [28–34]. The helium atom is a fundamental, conceptually clean and experimentally accessible system which can be used to shed some light onto this subject.

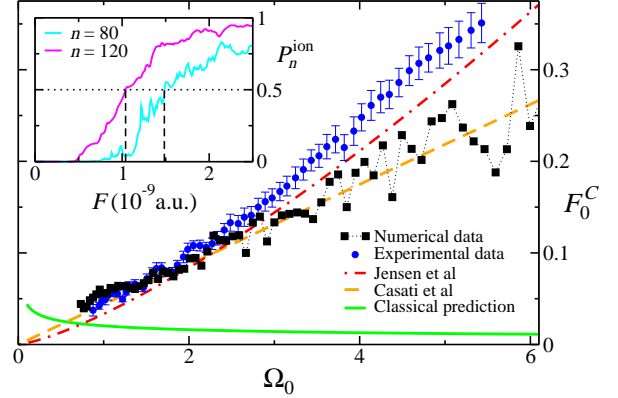


FIG. 1. (color online) Scaled critical fields $F_0^C = n^4 F^C$ vs scaled frequencies $\Omega_0 = n^3 \omega$ ($\omega = 2.667 \times 10^{-6}$ a.u.), for the second Rydberg series of Zee helium: $N = 2$ and $n \in [65, 130]$. Our numerical data for helium are indicated by black squares. Experimental results for Sr are reproduced from Ref. [21]. The dashed line marks the prediction for 1D hydrogen given by Casati *et al.* [19]. The dashed-dotted line indicates the result given by Jensen *et al.* [17]. The solid line corresponds to the classical prediction [19]. The inset shows ionization yield P_n^{ion} vs field strength F for two states $n = 80, 120$. Vertical lines mark the required critical fields to yield 50% ionization after a driving time of 20 ns.

Field-free helium.— We consider two distinct configurations of collinear helium, namely Zee and eZe helium, characterized by whether the electrons are located on the same side or on opposite sides of the nucleus, which is fixed at the origin. The field-free Hamiltonian in atomic units reads

$$H_0 = \frac{1}{2} (p_1^2 + p_2^2) - \frac{Z}{r_1} - \frac{Z}{r_2} + \frac{\gamma}{r_{12}}, \quad (1)$$

for $Z = 2$, where $r_1, r_2 > 0$ denote the radial coordinates of the electrons, and $r_{12} = |r_1 \mp r_2|$ for $Zee(-)$ and $eZe(+)$ helium [35]. The momentum operators are defined with respect to the radial coordinates only, $p_j \equiv -i\partial_{r_j}$. The parameter γ , with a physical value $\gamma = 1$, is introduced to tune the strength of the electronic interaction. No transition can take place between both configurations due to the presence of the Coulomb

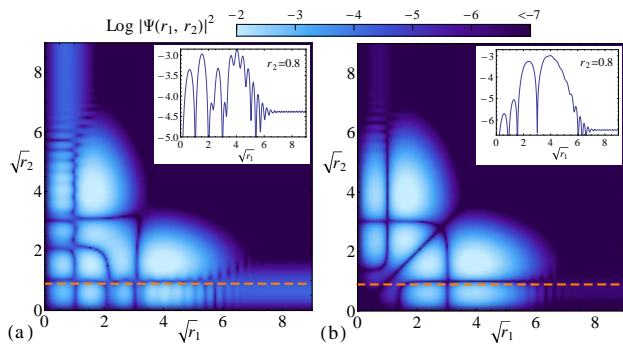


FIG. 2. (color online) Wavefunctions of eZe helium for (a) even and (b) odd states for $(N, n) = (2, 4)$. The energies and decay rates (E, Γ) are $(-0.553538, 1.681 \times 10^{-4})$ a.u. and $(-0.556019, 1.391 \times 10^{-6})$ a.u., respectively. The insets show the distributions along the cut $r_2 = 0.8$ (dashed line on the density plots). The plots illustrate a transition from a doubly bound to a single ionized part as one moves along one of the coordinate axes, which is more pronounced in the even case. The nodal line structure in the doubly bound regions reflect the quantum numbers and the symmetry of the states.

singularity at the origin. The classical dynamics underlying the two configurations are rather distinct and exhibit complementary features of the three-dimensional problem [36]. While the eZe phase space is fully chaotic [37], leading to fast fragmentation, stable ‘frozen planet states’ exist for Zee helium due to an adiabatic separation of timescales of the motions of the inner and outer electron [38–40].

The interaction term γ/r_{12} in H_0 induces a coupling of all doubly excited states to the underlying single-ionization continua, and thus turns them into resonances with finite decay (autoionization) rates. The energies E_j , decay rates Γ_j and wavefunctions ϕ_j associated to these resonances can be calculated from the eigenvalues and eigenstates of a non-hermitian Hamiltonian obtained by the method of complex rotation [41]. The complex-rotated Hamiltonian and all necessary operators are represented in the two-electron Hilbert space using a basis of Sturmian functions [39, 42]. In order to treat exactly all the Coulomb terms in Eq. (1) we work with a regularized H_0 , multiplied by $r_1 r_2 r_{12}$. The Schrödinger equation then translates into a generalized eigenvalue problem, involving sparse matrices, which we solve numerically [43].

The discrete spectrum of collinear helium can be characterized by quantum numbers (N, n) , and it is organized in Rydberg series which converge to single ionization thresholds $E_N = -Z^2 N^{-2}/2$ [40]. In a typical Rydberg state ($N = 2, n \sim 100$) we find autoionization rates for Zee -helium corresponding to high lifetimes $\tau_{\text{typ}} = \Gamma_{\text{typ}}^{-1} \sim 300 \mu\text{s}$, in accordance with the classical stability of this configuration. For eZe we obtain two sets of resonances, even and odd with respect to the exchange of r_1 and r_2 (cp. Fig. 2), with $\tau_{\text{typ}} \sim 5$ ns and

500 ns, respectively. The enhanced stability of the odd states can be understood from their vanishing close to the triple collision point $r_1 = r_2 = 0$ [38].

Driven helium.— We take into account a dipole coupling to an external classical electromagnetic field of strength F and frequency ω . The Hamiltonian in velocity gauge reads $H = H_0 + H_F$, where

$$H_F = \frac{F}{\omega}(p_1 \pm p_2) \sin(\omega t) = V_F \sin(\omega t), \quad (2)$$

for $Zee(+)$ and $eZe(-)$. Due to the periodicity of H_F , we may use Floquet theory to solve the time-dependent Schrödinger equation for the complex rotated Hamiltonian. The elementary solutions have the form

$$\psi_\epsilon(t) = e^{-i\epsilon t} \sum_{k=-\infty}^{\infty} e^{-ik\omega t} \psi_\epsilon^k, \quad (3)$$

where the Floquet components ψ_ϵ^k and quasienergies ϵ obey the eigenvalue equation

$$(H_0 - k\omega)\psi_\epsilon^k + \frac{1}{2i}V_F(\psi_\epsilon^{k+1} - \psi_\epsilon^{k-1}) = \epsilon \psi_\epsilon^k. \quad (4)$$

The Floquet index k can be effectively related to the number of photons exchanged between atom and field [46]. Given a reference state with energy E_0 , we expand the components ψ_ϵ^k in terms of field-free atomic eigenstates lying inside an energy interval ΔE , centered at $E_k = E_0 + k\omega$. The tolerance ΔE then corresponds to the maximum allowed detuning of any k -photon transition. We usually find well-converged results for $\Delta E < 10\omega$. Using this method, we reduce the dimensionality of the Floquet eigenvalue problem by three orders of magnitude, which enables us to consider processes of very high order (> 100) in k .

The field-induced transition probability between atomic levels ϕ_i and ϕ_j after an interaction time T with the field, is given by $P_{i \rightarrow j}(T) = |\langle \phi_j | U(T) | \phi_i \rangle|^2$, where the time evolution operator $U(T)$ is resolved in terms of the solutions in Eq. (3). The ionization probability of the initial atomic state ϕ_i is then obtained as $P_i^{\text{ion}}(T) = 1 - \sum_j P_{i \rightarrow j}(T)$.

For comparison with experimental data and theoretical predictions, we calculate ionization yields and critical fields F_0^C of Zee Rydberg states of the second series, $N = 2$, for the same parameters as those experimentally considered by Maeda and Gallagher for their measurements on Sr [21]. Due to the low excitation of the inner electron and the slow autoionization, we expect no crucial differences in comparison to driven hydrogen or alkali atoms. We use the scaled variables

$$F_0^C = n^4 F^C, \quad \Omega_0 = n^3 \omega, \quad (5)$$

to display the results: F_0^C is the critical field in units of the average Coulomb field in a hydrogen atom, and Ω_0 is

the frequency in units of the hydrogen level spacing. As shown in Fig. 1, our calculations for Zee helium—in spite of the one-dimensional nature of the model—agree with the experimental results of Ref. [21] in the regime $\Omega_0 \leq 2.5$. The deviations observed for larger Ω_0 might then be due to the dimensionality difference of the systems under comparison. Our data is also consistent with the localization-based prediction published in Ref. [19].

Influence of electron-electron interaction on dynamical localization.— The energy of a doubly excited state can be cast into an effective Rydberg form via

$$E = -\frac{Z^2}{2N^2} - \frac{Z_{\text{eff}}^2}{2n_{\text{eff}}^2}, \quad (6)$$

where $Z_{\text{eff}} = Z - \gamma$ and $\gamma \in [0, 1]$ controls the strength of the electron repulsion. The effective quantum number n_{eff} encodes the influence of the electron-electron interaction on the spectrum. For the Zee configuration we found that $n_{\text{eff}} = n + \delta_N$, given by a so-called quantum defect δ_N , which is only determined by the series index N . The whole spectrum of Zee helium is described very accurately by δ_N and Eq. (6) [47]. Following this picture, we argue that the outer electron sees a mean level spacing given by $\Delta = n_{\text{eff}}^{-3} Z_{\text{eff}}^2$ and experiences a Coulomb field $f = n_{\text{eff}}^{-4} Z_{\text{eff}}^3$. The critical ionization fields F^C and the driving frequency ω_γ should then be measured with respect to these fundamental quantities. The appropriately scaled variables in this case are

$$\tilde{F}_0^C \equiv \frac{F^C}{f} = n_{\text{eff}}^4 Z_{\text{eff}}^{-3} F^C, \quad \tilde{\Omega}_0 \equiv \frac{\omega_\gamma}{\Delta} = n_{\text{eff}}^3 Z_{\text{eff}}^{-2} \omega_\gamma. \quad (7)$$

The driving frequency is changed with γ as $\omega_\gamma = Z_{\text{eff}}^2 \omega_1$, where $\omega_1 = 1.5 \times 10^{-6}$ a.u. is a reference frequency corresponding to $\gamma = 1$ ($Z_{\text{eff}} = 1$). This scaling ensures that for a given value of $\tilde{\Omega}_0 = n_{\text{eff}}^3 \omega_1$ the number of photons needed to ionize the outer electron is the same for all γ . This latter condition is crucial to compare the occurrence of localization for different interaction strengths.

We first calculate the critical fields $F^C = F^{20\%}$ yielding 20% ionization after a driving time of 100 ns, of states in the second Rydberg series of Zee helium ($N = 2$) for different values of γ [50]. The obtained F^C are shown in the inset of Fig. 3. For a fixed $\tilde{\Omega}_0$, the critical field decreases by almost one order of magnitude with increasing γ . Therefore, the ionization process is strongly enhanced due to the electron-electron interaction, which in turn reflects a weakening of localization. Nevertheless, as seen in Fig. 3, the values of the scaled field \tilde{F}_0^C remarkably coincide for all γ up to fluctuations, indicating that the absolute critical fields F^C are proportional to Z_{eff}^3 . We found that this result carries over to the first Rydberg series ($N = 1$) of eZe helium, also shown in Fig. 3. We also considered the more interesting high series $N = 29$ for Zee helium. The electron-electron interaction is quantitatively very relevant in this case, as indicated by the

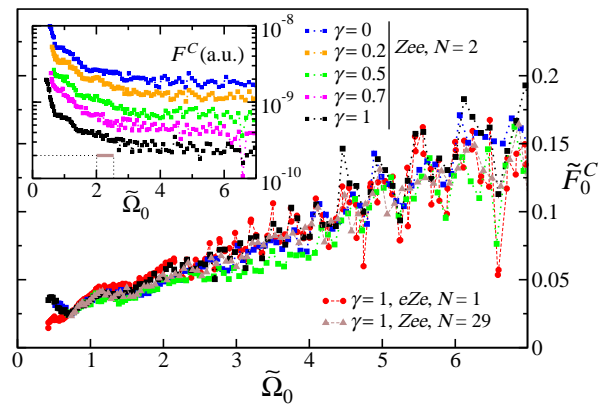


FIG. 3. (color online) Scaled critical fields $\tilde{F}_0^C = n_{\text{eff}}^4 Z_{\text{eff}}^{-3} F^C$ vs scaled frequencies $\tilde{\Omega}_0 = n_{\text{eff}}^3 Z_{\text{eff}}^{-2} \omega_\gamma = n_{\text{eff}}^3 \omega_1$ for 20% ionization after a driving time of 100 ns, for different series N and values of the interaction strength γ . The shown range of $\tilde{\Omega}_0$ corresponds to $n_{\text{eff}} \in [65, 170]$, and the number of absorbed photons needed for ionization ranges from 80 to 12. For $N = 2$ the quantum defect is negligible whereas $\delta_{N=2}^{Zee} \simeq 14$. The inset shows the absolute critical fields F^C vs $\tilde{\Omega}_0$ for $N = 2$ and Zee helium. The horizontal bar in the inset marks the parameter region considered for the simulations of Fig. 4.

value of the quantum defect $\delta_{N=29}^{Zee} \simeq 14$. As shown in Fig. 3, the scaled critical fields again coincide with the data for the low-lying series.

The collapse of the critical field curves suggests that the influence of the inner electron on the ionization dynamics can be understood from the appropriate rescaling of the level spacing and the elementary Coulomb field for the outer electron. In the case of doubly excited eZe states, however, fast autoionization makes the definition of critical fields meaningless. In order to show that dynamical localization is present, we monitor directly the field-induced transitions $P_{i \rightarrow j}(T)$ between atomic levels. The population redistribution of a driven initial state ϕ_i is then visualized in energy space as a function of the excitation energy $\Delta E = E_j - E_i$, measured in multiples $k \in \mathbb{Z}$ of the photon energy. The resulting populations $P(k)$ can thus be correlated to the net number of photons emitted and absorbed. Figure 4 shows these distributions for the second series of Zee and eZe , averaged over initial states $n \in [110, 119]$, for several driving times. The chosen field strength, $F = 2 \times 10^{-10}$ a.u., is strong enough to observe a considerable spreading, but still does not lead to ionization of the Zee initial states (see the bar in the inset of Fig. 3). In the Zee case the distribution freezes completely after about 10 ns and approaches an exponentially localized shape. For the eZe states, the distribution also reaches an exponential dependence on k , but its norm decreases with time due to fast autoionization, as seen in the upper inset of Fig. 4.

Although autoionization shifts the eZe distribution to smaller values, it seems to have no influence on its ex-

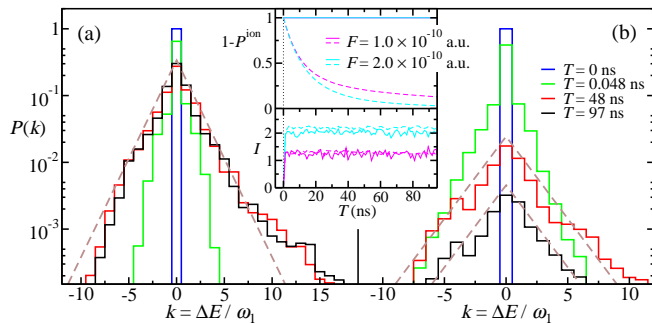


FIG. 4. (color online) Transition probabilities $P(k)$ vs excitation energy in units of ω_1 ($\gamma = 1$), averaged over initial states $n \in [110, 119]$ of the $N = 2$ Rydberg series of (a) Zee and (b) eZe helium, for a field strength of $F = 2 \times 10^{-10}$ a.u. (see corresponding $\tilde{\Omega}_0$ range in the inset of Fig. 3), after a driving time T . The bin size of the histograms is $\Delta k = 1$. Thick dashed lines highlight the exponential decay according to the localization length obtained from the analysis of the Shannon information, I . The upper and lower insets show respectively the probability of the outer electron to remain bound to the atom, $1 - P^{\text{ion}}$, and I of the normalized distributions vs T (dashed lines: eZe , solid lines: Zee), averaged over the same states and for two different field strengths. Fast autoionization of the eZe states is also observed for smaller fields of $F = 1 \times 10^{-10}$ a.u.. The averaged decay rates for the odd and even eZe states in the range considered for n are $\bar{\Gamma}_{\text{even}} = 3.3 \times 10^{-9}$ a.u. and $\bar{\Gamma}_{\text{odd}} = 3.1 \times 10^{-11}$ a.u.. For the Zee states $\bar{\Gamma}_{Zee} = 6.9 \times 10^{-14}$ a.u..

ponential dependence on k . To prove that the spreading comes to a halt, we characterize the width of the normalized distribution $\hat{P}(k)$ via the Shannon information, $I = -\sum_k \hat{P}(k) \log \hat{P}(k)$. As depicted in the lower inset of Fig. 4, I increases rapidly for short times and then fluctuates around some saturated value. Hence the field-induced transport on the energy axis freezes, and we conclude that localization is still present despite any loss of norm due to autoionization.

In order to carry out a quantitative analysis of the localization behavior, we estimate the localization length ξ of the distributions $P(k) \sim \exp(-|k|/\xi)$ from the limiting value of I , averaged over times between 48 and 97 ns [51]. For the range of initial states considered, the obtained values of ξ seem to be roughly independent of n up to fluctuations caused by the local detuning of the field-induced transitions. The independence of ξ on n was also observed for driven hydrogen in Ref. [15]. The estimate of the localization length and its uncertainty are obtained from the average over initial states $n \in [110, 119]$. We studied the dependence of ξ on the field strength F for the second Rydberg series of both helium configurations, as well as its dependence on the interaction strength γ for Zee helium. As shown in the inset of Fig. 5, for a fixed field strength ξ increases with γ , once more demonstrating the enhancement of the excitation process due to the interaction. For a fixed γ the localization length

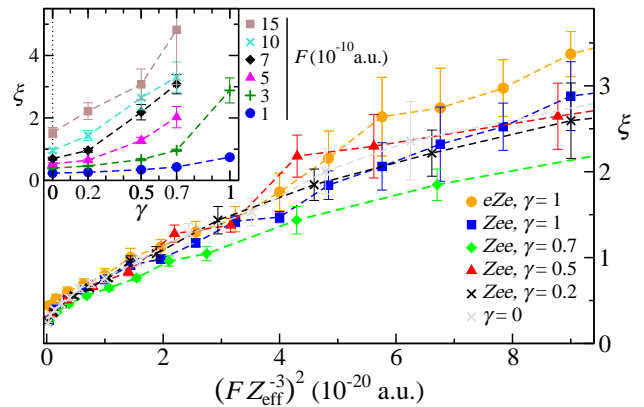


FIG. 5. (color online) Localization length ξ for the $N = 2$ Rydberg series of Zee and eZe helium, obtained from the Shannon information I of the distributions $P(k)$ [cp. Fig. 4], as a function of $(FZ_{\text{eff}}^{-3})^2$. An average of I for $T \in [48, 97]$ ns and over initial states $n \in [110, 119]$ has been considered. Error bars indicate one standard deviation. Higher F implies larger fluctuations of ξ as a function of n , which results in larger uncertainties. The inset shows ξ vs interaction strength γ for Zee states and several field intensities F .

also grows with the field strength F [52]. As discussed above, the critical fields scale with Z_{eff}^3 . Therefore, in order to treat different interaction strengths on an equal footing, we should rescale F . As shown in Fig. 5 the values of ξ as a function of FZ_{eff}^{-3} overlap within their 95% CI for all values of γ . Therefore, the influence of the electron-electron interaction on localization can be described by taking into account an appropriate rescaling of the field strength with the effective charge. Additionally, we observe that the estimated localization lengths are seemingly compatible with a quadratic scaling law, $\xi \sim (FZ_{\text{eff}}^{-3})^2$. The relation $\xi \sim F^2$ was found for driven hydrogen in Ref. [15].

In conclusion, using efficient numerical techniques we have verified the suppression of field-induced single-particle ionization in helium due to dynamical localization. We have shown that the effect of electron-electron interaction on localization can be described through the influence of the former on the atomic level density and an appropriate scaling of the external field with the effective charge. We have also observed localization for doubly excited states in the presence of fast autoionization as a dominant competing process. We emphasize that dynamical localization in the presence of autoionization is the equivalent of Anderson localization in the presence of absorption, which poses a challenge for the observation of light localization. The latter can be seen, irrespective of absorption, from the time dependence of the distribution width of transmitted-light through random media [53], in the same way we monitor the width of our normalized populations. This technique was used recently to provide what seems to be evidence of an Anderson transition for

light in three dimensions [54].

We thank Pierre Lukan for fruitful discussions and numerical support during the early stages of this project. The authors gratefully acknowledge the Deutsche Forschungsgemeinschaft (DFG) for financial support, and the computing time granted by the John von Neumann Institute for Computing (NIC), and provided on the supercomputer JUROPA at Jülich Supercomputing Centre (JSC). Numerical calculations were also performed on the Black Forest grid (BFG, Freiburg).

* abu@uni-freiburg.de

- [1] P. W. Anderson, Phys. Rev. **109**, 1492 (1958).
- [2] J. Billy *et al.*, Nature **453**, 891 (2008).
- [3] G. Roati *et al.*, Nature **453**, 895 (2008).
- [4] F. Jendrzejewski *et al.*, Nat. Phys. **8**, 398 (2012).
- [5] S. S. Kondov, W. R. McGehee, J. J. Zirbel, and B. DeMarco, Science **334**, 66 (2011).
- [6] H. Hu *et al.*, Nat. Phys. **4**, 945 (2008).
- [7] T. Schwartz, G. Bartal, S. Fishman, and M. Segev, Nature **446**, 52 (2007).
- [8] S. Fishman, D. R. Grempel, and R. E. Prange, Phys. Rev. Lett. **49**, 509 (1982).
- [9] F. L. Moore *et al.*, Phys. Rev. Lett. **73**, 2974 (1994).
- [10] J. Ringot, P. Szriftgiser, J. C. Garreau, and D. Delande, Phys. Rev. Lett. **85**, 2741 (2000).
- [11] J. Chabé *et al.*, Phys. Rev. Lett. **101**, 255702 (2008).
- [12] G. Lemarié *et al.*, Phys. Rev. Lett. **105**, 090601 (2010).
- [13] M. Lopez *et al.*, Phys. Rev. Lett. **108**, 095701 (2012).
- [14] M. Lopez *et al.*, New J. of Phys. **15**, 065013 (2013).
- [15] G. Casati *et al.*, Phys. Rev. A **36**, 3501 (1987).
- [16] J. E. Bayfield, G. Casati, I. Guarneri, and D. W. Sokol, Phys. Rev. Lett. **63**, 364 (1989).
- [17] R. V. Jensen, S. M. Susskind, and M. M. Sanders, Phys. Rev. Lett. **62**, 1476 (1989).
- [18] A. Schelle, D. Delande, and A. Buchleitner, Phys. Rev. Lett. **102**, 183001 (2009).
- [19] G. Casati, I. Guarneri, and D. Shepelyansky, IEEE J. Quantum Electron. **24**, 1420 (1988).
- [20] M. Arndt, A. Buchleitner, R. N. Mantegna, and H. Walther, Phys. Rev. Lett. **67**, 2435 (1991).
- [21] H. Maeda and T. F. Gallagher, Phys. Rev. Lett. **93**, 193002 (2004).
- [22] A. Krug and A. Buchleitner, Phys. Rev. Lett. **86**, 3538 (2001).
- [23] B. Deissler *et al.*, Nat. Phys. **6**, 354 (2010).
- [24] L. Pollet, N. V. Prokof'ev, B. V. Svistunov, and M. Troyer, Phys. Rev. Lett. **103**, 140402 (2009).
- [25] S. Anissimova *et al.*, Nat. Phys. **3**, 707 (2007).
- [26] I. L. Aleiner, B. L. Altshuler, and G. V. Shlyapnikov, Nat. Phys. **6**, 900 (2010).
- [27] L. Sanchez-Palencia and M. Lewenstein, Nat. Phys. **6**, 87 (2010).
- [28] W. Becker, X. Liu, P. J. Ho, and J. H. Eberly, Rev. Mod. Phys. **84**, 1011 (2012).
- [29] R. C. Bilodeau *et al.*, Phys. Rev. Lett. **111**, 043003 (2013).
- [30] Y. Zhou, C. Huang, Q. Liao, and P. Lu, Phys. Rev. Lett. **109**, 053004 (2012).
- [31] N. Camus *et al.*, Phys. Rev. Lett. **108**, 073003 (2012).
- [32] B. Walker *et al.*, Phys. Rev. Lett. **73**, 1227 (1994).
- [33] T. Weber *et al.*, Nature **405**, 658 (2000).
- [34] R. Moshhammer *et al.*, Phys. Rev. A **65**, 035401 (2002).
- [35] For *Zee* helium we may further assume $r_1 > r_2$ since due to the Coulomb repulsion the electrons cannot switch positions. In fact, in the (r_1, r_2) radial subspace we can consider the electrons as distinguishable particles in both configurations. Proper antisymmetric (symmetric) spatial wavefunctions in the full (\vec{r}_1, \vec{r}_2) space, corresponding to a triplet (singlet) spin configuration, can be constructed from the basic solutions obtained in the radial subspace.
- [36] A. López-Castillo, M. A. M. de Aguiar, and A. M. O. de Almeida, J. Phys. B: At. Mol. Opt. Phys. **29**, 197 (1996).
- [37] G. S. Ezra, K. Richter, G. Tanner, and D. Wintgen, J. Phys. B: At. Mol. Opt. Phys. **24**, L413 (1991).
- [38] K. Richter, G. Tanner, and D. Wintgen, Phys. Rev. A **48**, 4182 (1993).
- [39] P. Schlagheck and A. Buchleitner, J. Phys. B: At. Mol. Opt. Phys. **31**, L489 (1998).
- [40] G. Tanner, K. Richter, and J.-M. Rost, Rev. Mod. Phys. **72**, 497 (2000).
- [41] E. Balslev and J. Combes, Commun. Math. Phys. **22**, 280 (1971).
- [42] P. Schlagheck and A. Buchleitner, Eur. Phys. J. D **22**, 401 (2003).
- [43] We use the PETSc [44] and SLEPc [45] libraries.
- [44] Satish Balay *et al.*, <http://www.mcs.anl.gov/petsc>
- [45] V. Hernandez, J. E. Roman, and V. Vidal. ACM Trans. Math. Software **31**, 351 (2005).
- [46] J. H. Shirley, Phys. Rev. **138**, B979 (1965).
- [47] While the ansatz $n_{\text{eff}} = n + \delta_N$ is usually only valid asymptotically for $n \gg N$, it describes remarkably well the entire discrete spectrum of *Zee* helium, including $n \approx N$. We derive δ_N^{Zee} from a semiclassical analysis, after constructing an N -dependent effective potential for the outer electron following Refs. [48, 49]. We find $\delta_N^{Zee} \simeq -1/2 + 0.49 N$, where the coefficient of N results from the semiclassical quantization for $N = 1$, that we performed numerically. The magnitude of the numerical deviation between n_{eff} estimated from the energy and that obtained from δ_N^{Zee} was always smaller than 0.1 for the range of states considered.
- [48] V. N. Ostrovsky and N. V. Prudov, J. Phys. B: At. Mol. Opt. Phys. **28**, 4435 (1995).
- [49] P. Schlagheck, Ph.D. thesis, TU München, 1999.
- [50] A driving time of 100 ns for the frequency ω_γ corresponds to $\sim 10^3 Z_{\text{eff}}^2$ periods.
- [51] The relation between ξ and I follows by calculating the Shannon information for a perfect exponentially decaying normalized distribution. By inverting numerically the resulting expression we obtain ξ for any value of I .
- [52] For the estimation of ξ we must work with field strengths below the critical values of the *Zee* states involved, $F Z_{\text{eff}}^{-3} \approx 3 \times 10^{-10}$ a.u.. For higher fields the increasing overlap of the distributions with single continuum states at the ionization threshold distorts the exponentially localized shape.
- [53] N. Cherroret, S. E. Skipetrov, and B. A. van Tiggelen, Phys. Rev. E **82**, 056603 (2010).
- [54] T. Sperling, W. Buhrer, C. M. Aegerter, and G. Maret, Nat. Photon. **7**, 48 (2013).